Stereoscopic imaging of an Earth-impacting solar coronal mass ejection: A major milestone for the STEREO mission

C. J. Davis,[1] J. A. Davies,[1] M. Lockwood,[1,2] A. P. Rouillard,[1,2] C. J. Eyles,[1] and R. A. Harrison[1]

Received 4 March 2009; revised 19 March 2009; accepted 23 March 2009; published 18 April 2009.

[1] We present stereoscopic images of an Earth-impacting Coronal Mass Ejection (CME). The CME was imaged by the Heliospheric Imagers onboard the twin STEREO spacecraft during December 2008. The apparent acceleration of the CME is used to provide independent estimates of its speed and direction from the two spacecraft. Three distinct signatures within the CME were all found to be closely Earth-directed. At the time that the CME was predicted to pass the ACE spacecraft, in-situ observations contained a typical CME signature. At Earth, ground-based magnetometer observations showed a small but widespread sudden response to the compression of the geomagnetic cavity at CME impact. In this case, STEREO could have given warning of CME impact at least 24 hours in advance. These stereoscopic observations represent a significant milestone for the STEREO mission and have significant potential for improving operational space weather forecasting. **Citation:** Davis, C. J., J. A. Davies, M. Lockwood, A. P. Rouillard, C. J. Eyles, and R. A. Harrison (2009), Stereoscopic imaging of an Earth-impacting solar coronal mass ejection: A major milestone for the STEREO mission, *Geophys. Res. Lett.*, *36*, L08102, doi:10.1029/2009GL038021.

1. Introduction

[2] The region of influence of the Sun's atmosphere, the heliosphere, extends beyond Earth and indeed all of the planets in our solar system. The heliosphere is a hazardous radiation environment. In particular solar energetic particles (SEPs), which are accelerated by the shock situated at the leading edge of coronal mass ejections (CMEs), are a major hazard to spacecraft systems and astronauts [e.g., *Reames*, 1999; *Lockwood*, 2007; *Lockwood and Hapgood*, 2007]. Predicting both the occurrence and the trajectory of CMEs is therefore crucial in characterizing the radiation hazards at specific locations in the heliosphere – with Earth being of particular importance.

[3] The structure of a CME is characteristically in three parts, with a leading density front followed by a dense core often identified as prominence material, separated by a plasma void. Within this cavity is often embedded a helical magnetic field structure termed a magnetic flux rope.

[4] CMEs are mainly imaged in white light – sunlight that has been Thomson scattered from CME-associated electrons [e.g., *Billings*, 1966; *Vourlidas and Howard*, 2006]. As the electrons preferentially Thomson scatter the sunlight through 90°, this mechanism favors the observation of plasma lying close to the surface of a sphere where the observer and the Sun lie at opposite ends of a diameter. Most CME imaging has been performed from spacecraft located at the first Lagrangian point such as the Solar Heliospheric Observatory, SOHO [*Domingo et al.*, 1995] or from Earth orbit such as the P78-1 spacecraft [*Doschek*, 1983] or the Solar Maximum Mission [*MacQueen et al.*, 1980] and, more recently, the Solar Mass Ejection Imager, SMEI, on the Coriolis mission [*Eyles et al.*, 2003]. Due to the nature of Thomson scattering, Earth-directed CMEs are best viewed from a vantage point well away from the Sun-Earth line. The NASA STEREO mission [*Kaiser et al.*, 2008] was designed to achieve this. Launched on October 25th 2006, this mission placed two almost identical solar observatories into Earth-like orbits, one ahead of the Earth (spacecraft A) and the other behind the Earth (spacecraft B). The spacecraft are drifting away from the Earth at a rate that increases each spacecraft-Sun-Earth angle by 22.5° per year. Their positions in December 2008 are shown in Figure 1. As part of a comprehensive suite of remote-sensing and in-situ instrumentation, each spacecraft carries a Heliospheric Imager (HI), consisting of two cameras; the inner camera (HI-1) has a 20° field of view centered at 14° elongation from Sun centre while the outer camera (HI-2) has a 70° field of view centered at 53.7° from Sun centre. The combined HI field of view [*Eyles et al.*, 2009] enables CMEs to be tracked through elongations ranging from 4° to 88.7°. As the mission has evolved, the Earth has entered the HI-2 field of view. The purpose of our study is to use stereoscopic observations to prove the efficacy of the established techniques in determining the speed and direction of a CME and to show that such measurements have direct application to space weather forecasting.

2. Observations

[5] At the time of the observations presented in this paper, the two STEREO spacecraft were separated by an angle of 89.45°. Venus and Earth were visible in the HI images from STEREO-A, while the Earth was visible in the STEREO-B images (Figure 1). As well as detecting scattered light from coronal electrons, the HI cameras are sensitive to sunlight scattered from dust – the F-corona – and any stars and planets in the field of view. As the intense F-coronal signal remains constant on timescales far longer than the cadence of the HI images (40 and 120 minutes for HI-1 and HI-2, respectively) it can be effectively removed

[1]Space Science and Technology Department, Rutherford Appleton Laboratory, Chilton, UK.
[2]Space Environment Physics Group, University of Southampton, Southampton, UK.

0094-8276/09/2009GL038021$05.00

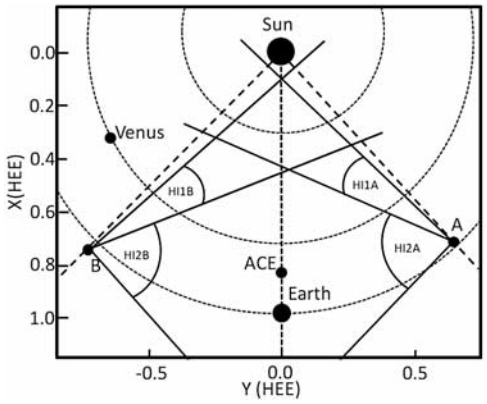

Figure 1. A projection onto the ecliptic plane showing the positions of the STEREO spacecraft (in Heliocentric Earth Ecliptic coordinates) with respect to the Earth at the time of the observations presented. The total separation angle of the spacecraft (A-Sun-B) was 89.45°. The fields of view of the HI cameras are shown.

by either subtraction of a long-term background or by the running difference technique. The latter is used particularly to reveal faint features propagating through the field of view. Figure 2 shows a CME observed in the HI cameras on both STEREO-A and STEREO-B spacecraft during December 2008. Such stereoscopic images of an Earth-directed CME represent the achievement of a major objective of the STEREO mission.

[6] CMEs are generally considered to have undergone initial acceleration before they reach the elongations covered by the HI cameras [*Vršnak et al.*, 2007]. By making the assumption that a CME is travelling at a constant velocity as it crosses the HI field of view, it is possible to fit the apparent acceleration/deceleration observed in the elongation variation to estimate its radial speed and angle of propagation with respect to the observer [*Sheeley et al.*, 1999, 2008a, 2008b; *Rouillard et al.*, 2008; *Davies et al.*, 2009]. Such a technique is not applicable to traditional coronagraph images since the CME may still be accelerating this close to the Sun and moreover the effect is negligible over the elongation range covered by coronagraphs.

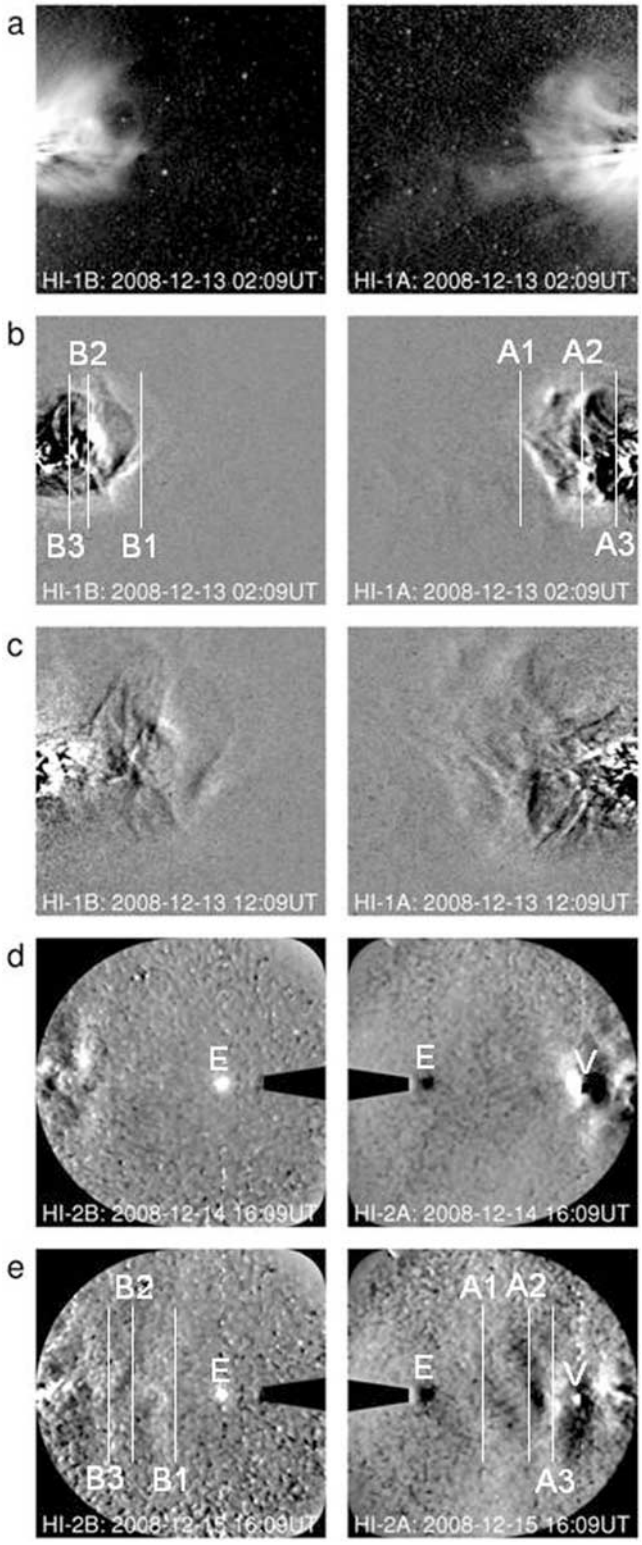

Figure 2. STEREO HI images through the evolution of the CME as observed from spacecraft A and B. Pairs of images correspond to near-simultaneous images from the two spacecraft, with images from B and A being plotted in the left- and right-hand columns, respectively. (a) The background-subtracted images from HI-1 reveal what appears to be two regions of enhanced intensity (density) separated by a void as would be expected in Thomson-scattered images of a typical CME. As the plasma densities in the CME decrease as it expands though the heliosphere, its white-light signature fades. Thus, at subsequent times during CME propagation, difference images are presented. (b) Running difference images corresponding to the background-subtracted images in row (a) for comparison. (c) Running difference HI-1 images some hours later, and (d and e) running difference images derived from HI-2. Regions of the HI-2 field of view obscured by the stray-light baffle system and Earth occulter are masked out. The features of the CME structure tracked are labeled as 1, 2, 3 (prefixed by the spacecraft A or B). These correspond to the leading density enhancement, the subsequent void and a second density enhancement. The position of Venus and Earth are labeled as V and E.

Table 1. Speed, Direction, and Predicted Arrival Times for the CME Features Observed in the HI Cameras

Spacecraft	Speed (kms^{-1})	CME-Sun-Earth Angle	Predicted Arrival at ACE (UT)	Predicted Arrival at Earth (UT)
A1	411 ± 23	−15 ± 13°	2008-12-16 11:21 (±3:00)	2008-12-16 12:23 (±3:00)
A2	360 ± 12	−4 ± 10°	2008-12-17 01:23 (±2:30)	2008-12-17 02:32 (±2:00)
A3	332 ± 6	−8 ± 5°	2008-12-17 13:07 (±1:15)	2008-12-17 14:22 (±1:15)
B1	417 ± 15	13 ± 7°	2008-12-16 08:36 (±2:00)	2008-12-16 09:36 (±2:00)
B2	351 ± 8	0 ± 7°	2008-12-17 04:25 (±1:15)	2008-12-17 05:36 (±1:15)
B3	331 ± 7	2 ± 7°	2008-12-17 10:47 (±1:15)	2008-12-17 12:03 (±1:15)

[7] The results of applying this fitting technique to three prominent features in the CME structure seen in HI images (marked on Figure 2) are summarized in Table 1. The first and third features correspond to enhanced intensity fronts while the second is the leading edge of the void between the two fronts. The agreement between the speeds and directions derived for each feature from the two spacecraft is very close. The independent observations provide a good validation of the technique and assumption of constant velocity. The small difference between the estimates of the direction of CME propagation from the two spacecraft is unsurprising since the spacecraft, situated on opposite sides of the CME, were undoubtedly imaging slightly different regions of the CME structures. Having estimated speeds and directions for the observed features within the CME, it is possible to predict arrival times at Earth. At these derived speeds, it will have passed over the Advanced Composition Explorer (ACE) spacecraft [*Stone et al.*, 1998], located 1.5 million km upstream of Earth, roughly 1 hr before it reached Earth. ACE interplanetary magnetic field and solar wind data are presented in Figure 3, along with the predicted arrival times at ACE of the three CME features tracked in the HI images.

[8] The ACE observations around the predicted times are indeed characteristic of a CME, with a magnetic flux rope - identified by a smooth rotation in the magnetic field components (Figure 3e) accompanied by an increase in the field magnitude (Figure 3d) - embedded within, but towards the trailing edge of, a region of enhanced plasma density (Figure 3a). The flux rope itself is associated with a plasma cavity, the elevated magnetic pressure acting to evacuate the particle population within. The increased density leading the structure, and that at the trailing edge of the flux rope, correspond to the leading front and the core material of the CME, respectively. These two regions of enhanced density correspond to the two bright regions imaged by HI. The predicted arrival times at ACE of the first and third HI-imaged features match well the times at which these features are seen in situ. Feature 2 is the trailing edge of the first density front imaged by HI and also corresponds to the in-situ observation. ACE observes weakly enhanced solar wind speeds during the passage of the CME which correspond well with the event motion speeds estimated from the HI images. The speed differential between the three measured CME features is evidence that the CME was still expanding as it passed ACE.

[9] Approximately an hour after the arrival time of the leading CME density front at ACE, a positive enhancement was observed in the horizontal component of the Earth's magnetic field, detected by all mid- to low-latitude dayside ground-based magnetometer stations at European and African longitudes (shown individually in Figure 4a and averaged in Figure 4b). This sudden impulse signature, seen near 08:00 UT on 16th December, is consistent with a compression of the dayside geomagnetic field in response to a sharp increase in the solar wind dynamic pressure

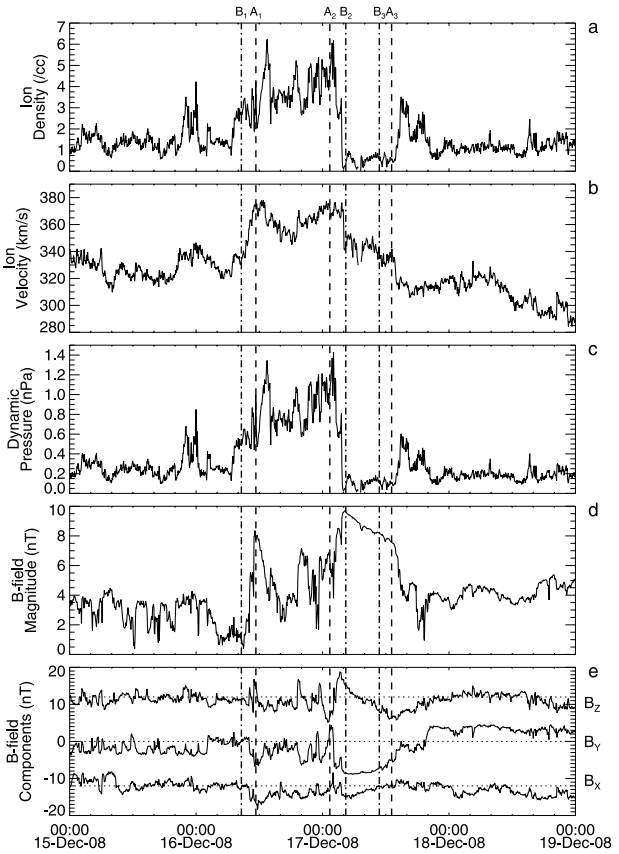

Figure 3. ACE solar wind and interplanetary magnetic field observations during the period 15th December to 19th December, 2008. (a) Ion number density and (b) the bulk velocity from the ACE/SWEPAM instrument. (c) Solar wind dynamic pressure derived therefrom. (d) Magnetic field magnitude $|\mathbf{B}|$ from the ACE/MAG instrument. (e) Components of $\mathbf{B}$ in Geocentric Solar Ecliptic coordinates. For clarity, the X and Z components of the field are offset by −12 and 12 nT, respectively. Note that although these are preliminary browse data, they are highly consistent with equivalent measurements from the Wind spacecraft relatively close-by; the two spacecraft do, however, exhibit a discrepancy in terms of their absolute densities. Dashed and dot-dashed lines plotted on all plots correspond to the times at which the three salient CME boundaries, observed by the two STEREO spacecraft, are predicted to pass over the ACE spacecraft.

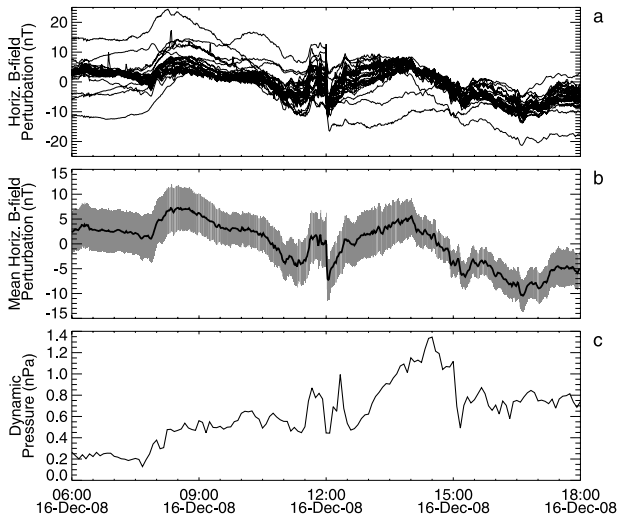

Figure 4. The response of the Earth's magnetic field. (a) The horizontal magnetic field component from 29 equatorial and mid-latitude ground magnetometer stations, over the interval extending from 06 until 18 UT on 16th December 2008. Their locations, within Europe and Africa, mean that these magnetometers were on the dayside during this interval. Baselines of the mean over the interval presented have been subtracted from the traces. (b) The mean of the individual traces (solid black line) bounded by $\pm 1\sigma$ (shaded grey). (c) The solar wind dynamic pressure from Figure 3c over the same interval, lagged by 60 minutes to account for propagation time from the spacecraft to Earth.

(Figures 3c and 4c), resulting mainly from an increase in plasma concentration within the CME. When lagged by 60 minutes to account for propagation to Earth, sudden increases in the dynamic pressure within the initial density front match transient rises in the H component of the Earth's field. At around midnight on the 17th December 2008, the Ap geomagnetic index increased to 12 (from a background level around 4–6) in response to several modest substorms that were triggered at this time, likely associated with the reversal to negative of the IMF Bz component within the flux rope.

[10] Back-projection of the STEREO-HI data, assuming some early acceleration, suggests that the signatures of the CME onset at the Sun would be observed sometime between 04:00 and 08:00 UT on the 12th. NOAA reported a prominence eruption centered near N50, W15 that lifted between 06:00 and 08:00 UT and noted that, consistently, the SOHO/LASCO C2 coronagraph detected a slow CME off the NW limb seen initially at 09:30 UT. No geomagnetic activity warning was given as the eruption appeared to be directed well away from Earth.

[11] However, due to its location, the true nature of the erupting prominence is better viewed from STEREO-A – in particular in the EUVI He II 304 Angstrom emission line characteristic of chromospheric material. Prior to 04:00 UT, the EUVI-A images show the lifting of a high-latitude prominence arcade. A subsequent, major eruption along the arcade generates a finger-like extension reaching high into the corona. This feature extends to progressively lower latitudes, taking the form of a large arch.

[12] Observations from the STEREO-A COR2 coronagraph are consistent with this interpretation, showing an eruption of material to the north of and just prior to a subsequent CME eruption occurring approximately along the ecliptic. From these observations the CME speed was estimated at 340 kms^{-1} (although this is not the true velocity since it is projected into the plane of the sky).

[13] The HI images suggest that the CME consists of two loops. The simplest interpretation is that the inner loop is populated with this prominence material, originating from the northern leg of the event at onset. Helium was detected as this front passed the ACE spacecraft (not shown) which matches this interpretation. The outer CME loop is formed due to the expansion of the pre-existing coronal magnetic structure into the confines of which the prominence is erupting. The dominance of protons in this initial front confirms its coronal origin.

3. Discussion and Conclusions

[14] We have shown that the unique positioning of the STEREO spacecraft enabled this event to be tracked through the heliosphere and, with the techniques outlined in this paper and references therein, it was possible to identify this CME as Earth-directed, notwithstanding the NOAA forecast, and predict the arrival time at the position of the ACE spacecraft and Earth to an accuracy of a few hours. This is an exciting result but a statistical analysis of similar events and a comparison with current models is needed before we can ascertain the effectiveness of such a technique when applied to space-weather forecasting.

[15] While there are other radiation hazards in space, solar energetic particles (SEPs) around CME fronts represent a particular threat to astronauts since the mass spectrum of SEPs contains heavier ions (up to Fe ions). It is the interaction with these heavy ions that cause the most damage to biological molecules such as DNA [*Antonelli et al.*, 2004]. In this case, the CME shock front is too weak to generate significant SEP fluxes (only a few energetic Helium ions were detected) but STEREO could have given warning of the timing and potential fluxes at least 24 hours in advance (earlier with less precision). If mankind is to embark on the colonization of the Moon or send a manned mission to Mars or, indeed, send astronauts anywhere outside the protective shield provided by Earth's magnetic field, an accurate forecast of the space environment will be vital to ensure their survival [*Lockwood and Hapgood*, 2007]. The observations presented here represent a milestone for the STEREO mission and offer exciting potential for any future space-weather forecast.

[16] **Acknowledgments.** The Heliospheric Imager (HI) instrument was developed by a collaboration which included the University of Birmingham and the Rutherford Appleton Laboratory, both in the UK, and the Centre Spatial de Liège (CSL), Belgium, and the US Naval Research Laboratory (NRL), Washington DC, USA. SECCHI project, led by NRL, involves additional collaborators from LMSAL, GSFC (USA), MPI (Germany), IOTA and IAS (France). The authors acknowledge N. Ness at Bartol Research Institute and D. J. McComas at Southwest Research Institute (both USA) for the ACE/MAG and SWEPAM observations, respectively, and CDAWeb for providing the data. The results presented in this paper rely on data collected at magnetic observatories. We thank the national institutes that support them and INTERMAGNET for promoting high standards of magnetic observatory practice (www.intermagnet.org).

Correspondence and requests for materials should be addressed to C. J. Davis. (chris.davis@stfc.ac.uk)

References

Antonelli, F., et al. (2004), DNA fragmentation induced by Fe ions in human cells: Shielding influence on spatially correlated damage, *Space Life Sci.*, *34*, 1353–1357.

Billings, D. E. (1966), *A Guide to the Solar Corona*, Academic, New York.

Davies, J. A., R. A. Harrison, A. P. Rouillard, N. R. Sheeley Jr., C. H. Perry, D. Bewsher, C. J. Davis, C. J. Eyles, S. R. Crothers, and D. S. Brown (2009), A synoptic view of solar transient evolution in the inner heliosphere using the Heliospheric Imagers on STEREO, *Geophys. Res. Lett.*, *36*, L02102, doi:10.1029/2008GL036182.

Domingo, V., V. Fleck, and A. I. Poland (1995), The SOHO mission: An overview, *Solar Phys.*, *162*, 1–37.

Doschek, G. A. (1983), Solar instruments on the P78-1 spacecraft, *Sol. Phys.*, *86*, 9–16.

Eyles, C. J., et al. (2003), The solar mass ejection imager (SMEI), *Sol. Phys.*, *217*, 319–347.

Eyles, C. J., et al. (2009), The Heliospheric Imagers on-board the STEREO mission, *Sol. Phys.*, *254*, 387–445.

Kaiser, M. L., et al. (2008), The STEREO mission: An introduction, *Space Sci. Rev.*, *136*, 5–16.

Lockwood, M. (2007), Fly me to the Moon?, *Nat. Phys.*, *3*, 669–671.

Lockwood, M., and M. Hapgood (2007), The rough guide to the Moon and Mars, *Astron. Geophys.*, *48*, 11–17.

MacQueen, R. M., et al. (1980), The High Altitude Observatory Coronagraph/Polarimeter on the Solar Maximum mission, *Sol. Phys.*, *65*, 91–107.

Reames, D. (1999), Solar energetic particles: Is there time to hide?, *Radiat. Meas.*, *30*, 297–308.

Rouillard, A. P., et al. (2008), First imaging of corotating interaction regions using the STEREO spacecraft, *Geophys. Res. Lett.*, *35*, L10110, doi:10.1029/2008GL033767.

Sheeley, N. R., Jr., J. H. Walters, Y.-M. Wang, and R. A. Howard (1999), Continuous tracking of coronal outflows: Two kinds of coronal mass ejections, *J. Geophys. Res.*, *104*, 24,739–24,767.

Sheeley, N. R., et al. (2008a), SECCHI observations of the Sun's garden-hose density spiral, *Astrophys. J.*, *674*, L109–L112.

Sheeley, N. R., et al. (2008b), Heliospheric images of the solar wind at Earth, *Astrophys. J.*, *675*, 853–862.

Stone, E. C., et al. (1998), The Advanced Composition Explorer, *Space Sci. Rev.*, *86*, 1–22.

Vourlidas, A., and R. A. Howard (2006), The proper treatment of coronal mass ejection brightness: A new methodology and implications for observations, *Astrophys. J.*, *642*, 1216–1221.

Vršnak, B., et al. (2007), Acceleration phase of coronal mass ejections: 1. Temporal and spatial scales, *Sol. Phys.*, *241*, 85–98.

J. A. Davies, C. J. Davis, C. J. Eyles, R. A. Harrison, M. Lockwood, and A. P. Rouillard, Space Science and Technology Department, Rutherford Appleton Laboratory, R25, Room I-04, Chilton OX11 0QX, UK. (c.j.davis@rl.ac.uk)